A Numerical Study on the Residual Stress Measurement Accuracy Using Inverse Eigenstrain Method

M. Honarpisheh*, H. Khanlari

Mechanical Engineering Department, University of Kashan, Kashan, Iran.

Article info

Abstract

Investigation of residual stresses is of crucial importance due to their effect on the performance of engineering components. Recently, inverse methods have been developed for determination of the residual stresses. Inverse eigenstrain method is one of the mentioned inverse methods. The inverse eigenstrain method, which is based on the eigenstrain theory, uses limited measurements of residual elastic strains obtained from the experimental tests. In this study, effective parameters on result accuracy obtained from the 2D inverse eigenstrain method in residual stresses measurement were investigated using numerical experiment. The results indicated that in the inverse eigenstrain method the accuracy of the results increases with increasing the basis functions order and the number of the points where displacement is measured. Additionally, the result accuracy increases selecting the appropriate basis functions. Moreover, in this paper the inverse eigenstrain method was applied for an actual part. The results showed that in the real conditions too, accurate results can be obtained by selecting the appropriate parameters of the inverse eigenstrain method.

Nomenclature

$\varepsilon_z^*(x)$	Eigenstrain z-direction component	F_i	Basis function
K_i^z	Unknown coefficients of the series terms	I	Moment of inertia
M_y	Minimum bending moment required to enter the plastic zone	M_p	Bending moment required to enter the entire beam into the plastic zone
c	Half the length of the beam cross-section	b	Width of the beam cross-section
σ_y	Yield strength of the beam material	σ'	Released stress during unloading
Y_Y	Elastic region	$d(x_j)$	Measured average displacements
x_j	Point in the line of displacement measurement	σ	Stress in the elastic zone of the beam during loading
$d(x_j)$	Obtained average displacement from inputting a known eigenstrain distribution	C_{ji}	Average displacement in the line of displacement measurement for a known eigenstrain distribution

1. Introduction

Residual stresses are self-equilibrating stresses which are generated in parts by many manufacturing processes such as welding, machining, casting, and metal forming. Residual stresses can cause undesirable effects on the part properties such as fatigue life, tensile strength, and dimensional stability. Therefore disre-

garding of the residual stresses in design may result in serious dangers. On the other hand, the residual stresses can be useful depending on their distribution. So some processes such as shot peening are implemented for creating the beneficial compressive residual stresses [1]. Therefore quantifying of the residual stresses is very important in engineering components.

Destructive and non-destructive methods are used to measure the residual stress in components. The hole-drilling [2,3], contour [4,5], slitting [6-9], and ring-core methods [10] are known as the destructive methods. The residual stresses in the engineering components are typically determined by two methods, which are experimental tests and modeling of process. However, there are considerable restrictions on both methods [11]. In recent years, inverse methods have been developed for determination of the residual stresses. Inverse eigenstrain method is one of the mentioned inverse methods. In the inverse eigenstrain method, limited measurements obtained from the experimental tests are used. This method which is based on the eigenstrain theory is in combination with measured residual elastic strains [12].

Hill (1996) introduced the general principles of the inverse eigenstrain method in his Ph.D dissertation [13]; this method was used for measurement of the residual stress in the welding process. The method was developed by Korsunsky (2005 & 2006), Dewald and Hill (2006) and Korsunsky et al. (2007) [14-17]. They used a least squares method for determination of unknown eigenstrain distributions from limited experimental data of the residual elastic strains. Subsequently, others applied the inverse eigenstrain method for the residual stress measurement in different samples and processes. Jun et al. (2009), song et al. (2012), and musinski and McDowell (2015) used the inverse eigenstrain method for the residual stress measurement for different shot-peened samples [18-20]. Luckhoo et al. (2009) and Jun et al. (2010) applied the inverse eigenstrain method for the residual stress measurement in friction stir welds of steel and aluminum plates, respectively [21,22]. Synchrotron X-ray diffraction was used for the residual elastic strain measurement. Song et al. (2009) measured the residual stresses around welds of an industrial part using the inverse eigenstrain method [23]. Achintha and Nowell (2011), Achintha et al. (2013) and Coratella et al. (2015) used the inverse eigenstrain method for measuring the residual stress in their research for laser shock peening process [24-26]. Kartal et al. (2012 & 2015) utilized the inverse eigenstrain method for specifying the micro residual stress components in a single-crystal superalloy; The electron backscatter diffraction was used for measuring the residual elastic strains [27,28]. Kartal et al. (2015) applied the inverse eigenstrain method for investigation of the effect of technical and geometric parameters on the residual stresses in the welding of thick plates [29].

To evaluate the accuracy, they compared the results of inverse eigenstrain and contour methods. Similar to the contour method, they used the measured displacements obtained from cutting the plate in the inverse eigenstrain method. Ogawa and Ishii (2016) applied the 3D inverse eigenstrain method for measuring the weld residual stresses using measurements of the X-ray diffraction [30]. Fransen (2016) estimated the residual stresses resulting from selective laser melting for line, a layer, and ten layers using the 3D inverse eigenstrain method [31]; the estimated residual stresses were compared with the results of numerical method using the mentioned approach. It was emphasized on accuracy of the inverse eigenstrain method results.

In this paper, the influence of the 2D inverse eigenstrain method parameters on the result accuracy was investigated for the residual stress measurement using numerical experiment. Furthermore, for validation of the inverse eigenstrain method in real condition, this method was applied for an actual part.

2. Inverse Eigenstrain Method

Eigenstrain is an expression used to describe a discordant strain field in a part, which results from nonelastic processes such as cold working, welding, heat treatment etc. [29]. Eigenstrain causes residual stress in the part [28]. If the generated elastic strains in the parts are combined with the discordant eigenstrain, total strain compatibility is satisfied [29]. Moreover, the residual stresses caused by the elastic strains must satisfy equilibrium. The residual stresses are related to the elastic strains by Hooke's law. If the eigenstrain distribution is specified, the corresponding residual stresses and elastic strains can be obtained almost straight. However, the elastic strains (or displacements) are measured at limited points practically. Therefore, an inverse eigenstrain problem solution is needed to determine an unspecified eigenstrain distribution using the elastic strains or displacements [29]. In the following section, equations for determination of the unknown eigenstrain distribution for a 2D part using the inverse solution are stated in summary. For more detailed explanation, it is recommended referring to ref. [16].

Consider a 2D part which is worked by a continual process in the z-direction (Fig. 1) [16]. In the part, just the eigenstrain z-direction component, $(\varepsilon_z^*(x))$, generates the residual stresses. Once the eigenstrain distribution $(\varepsilon_z^*(x))$ is obtained, the residual stresses, $(\sigma_x(x,z))$, $(\sigma_z(x,z))$ and $(\tau_{xz}(x,z))$, can be calculated anywhere in the part.

Assume that $(\varepsilon_z^*(x))$, which is unknown, can be

stated as a series expansion:

$$\varepsilon_z^*(x) = \sum_{i=2}^{n} K_i^z F_i(x) \tag{1}$$

where F_i is known basis function which can be Legendre or Chebyshev polynomials and Kis are $n-1$ unknown coefficients of the series terms. The first two orders of the polynomial terms are eliminated. Because the mentioned orders necessarily satisfy compatibility and do not generate residual stress. According to Eq. (1), the problem of determination of the unknown eigenstrain distribution is limited to discovering K_i. These coefficients are found with an elastic inverse solution using the measured displacements. The measurement procedure of displacements in the inverse eigenstrain method is similar to that in the contour method. The part is cut from the middle and then the resulting displacements in the cutting plane are measured. The best devices for cutting and the displacement measurement are wire cut EDM and CMM, respectively. To remove the shear stresses effects and cutting errors the displacements from two half of the cut are averaged. For more explanation about the measurement procedure of displacements, it is recommended referring to ref. [4].
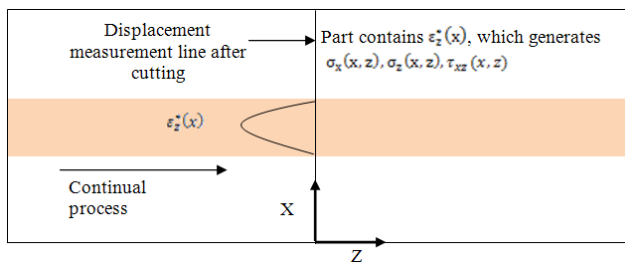

Fig. 1. Schematic of 2D part for description of the inverse eigenstrain method [16].

According to superposition principle, the measured average displacements can be stated as following:

$$\tilde{d}(x_j) = \sum_{i=2}^{n} K_i^z C_{ji} \tag{2}$$

where C_{ji} is the average displacement at point x_j in the line of displacement measurement (Fig. 1) for a known eigenstrain distribution $\varepsilon_z^*(x) = 0.001 F_i(x)$:

$$C_{ji} = d(x_j)||_{\varepsilon_z^*=0.001F_i(x)} \tag{3}$$

where $d(x_j)$ is an obtained average displacement from inputting a known eigenstrain distribution. To fit the values of input known eigenstrain with the measured values, $F_i(x)$ is multiplied by 0.001. C_{ji} can be obtained by finite element (FE) method. One half of the

cut part is modeled in an FE software. Then the known eigenstrain distribution is entered into the model. After the numerical solution, the displacements are extracted at the points which their displacements were measured in the experiment. This procedure continues for all $F_i(x)$. After the procedure is completed, a matrix is obtained with j (measurement points number) rows and $n-1$ columns. The mentioned matrix is named the compliance matrix. Eq. (2) is expressed in the matrix form as below,

$$\{\tilde{d}\} = [C]\{K\} \tag{4}$$

where,

$$\{\tilde{d}\} = [\tilde{d}(x_1), \tilde{d}(x_2), \cdots, \tilde{d}(x_j)]^T \tag{5}$$

and

$$\{K\} = [K_2^z, K_3^z, \cdots, k_i^z]^T \tag{6}$$

If the measurement points number, j, is more than the polynomial terms number, $i-1$, least squares can be used for calculation $\{K\}$:

$$\{K\} = ([C]^T[C])^{-1}[C]^T\{\tilde{d}\} \tag{7}$$

When K_i are specified, $\varepsilon_z^*(x)$ can be computed by Eq (1). Then $\varepsilon_z^*(x)$ is entered into an FE model of the initial part. After the numerical solution, the part residual stresses can be obtained.

3. Numerical Analysis

For investigating the effect of the inverse eigenstrain method parameters on the result accuracy in the residual stress measurement, a numerical experiment was performed. The main advantage of the numerical experiment is obtaining data without any errors which generally occurs in a real experiment such as cutting error [16]. In this research, for the numerical experiment and also for the inverse eigenstrain method, the numerical simulation software of ABAQUS 2016 was used.

In the beginning of the numerical experiment, the considered part must be modeled. In this regard, a beam was considered with rectangular cross-section of 50×120mm and length of 250mm (Fig. 2). The beam was assumed to be elastoplastic with yield strength of 250MPa, Young's modulus of 200GPa and Poisson's ratio of 0.33. In the first step of simulation, a bending moment with magnitude of 36.8KN.m was applied to the beam. In the next step, the applied moment was unloaded from the beam.
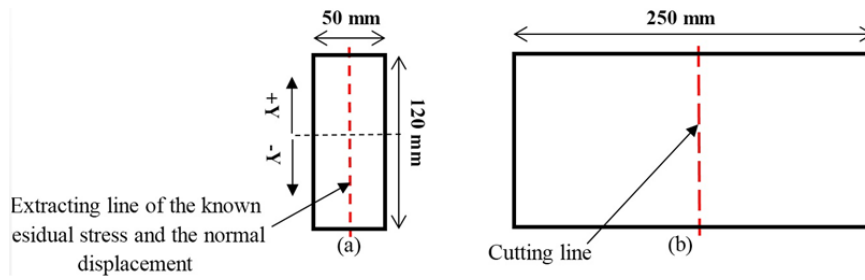
Fig. 2. Dimensions of the modeled beam used in numerical experiment a) Cross-section b) Longitudinal section.

After numerical solution, the longitudinal stresses in the normal direction on cross-section along the mid-line (Fig. 2a) were extracted for comparison with the calculated residual stresses by the inverse eigenstrain method. Henceforth, the mentioned longitudinal residual stresses will be called the known residual stresses. In the next step of numerical experiment, the FE model was cut into two parts from the middle (Fig. 2b) and the normal average displacements in the mid-line of the beam cross-section were extracted (Fig. 2a).

Since the known residual stresses and the displacements were obtained only in the mid-line of the beam cross-section (Fig. 2b), the steps of the inverse eigenstrain method were performed only for the longitudinal section of the beam at the mid-line of the cross-section.

After obtaining the average displacements from elastic cutting, the compliance matrix must be constituted. In this regard, the known eigenstrain distributions ($\varepsilon_z^*(x) = 0.001F_i(x)$) were entered into the FE model (one half of initial part) (Fig. 3) and after the numerical solution, the average displacements in the cutting line were extracted [Eq. (3)]. Then the basis functions coefficients were computed from Eq. (7). Finally, the calculated eigenstrain distribution [Eq. (1)] was entered into the FE model of the initial part (Fig. 4) and after solving of the FE problem, the resulting stresses were extracted as the estimated residual stresses by the inverse eigenstrain method.
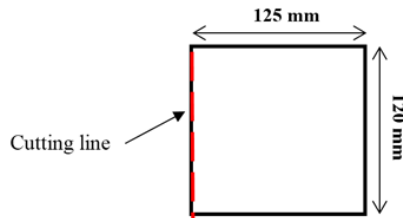

Fig. 3. 2D FE model for constitution of the compliance matrix in the inverse eigenstrain method.

4. Analytical Method

In this study, for verification of the FE simulation, an analytical method was also used to obtain the residual stresses of the beam under pure bending.
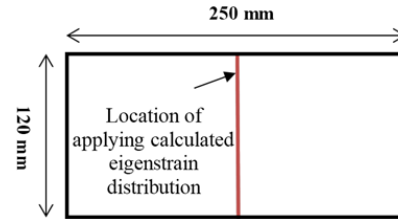

Fig. 4. The FE model for applying the calculated eigenstrain method in the 2D inverse eigenstrain method.

For explanation of the analytical method, the cross section of the beam with the mentioned specification in the numerical experiment section is again shown in Fig. 5.

The residual stress distribution of the beam after unloading is obtained of the following calculations:
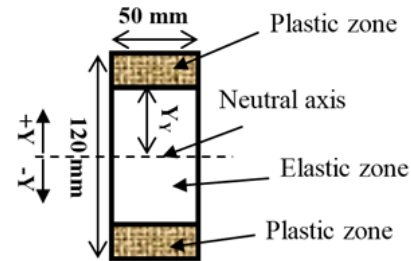

Fig. 5. The cross-section of the considered beam in this paper for description of analytical method.

The minimum bending moment required to enter the plastic zone, (M_y), is obtained from the following equation:

$$M_y = \frac{I}{c}\sigma_y = \frac{2}{3}(bc^2\sigma_y) \qquad (8)$$

where I is the moment of inertia of the beam cross-section, c is half the length of the beam cross-section (Fig. 5) (60mm), b is the width of the beam cross-section (Fig. 5) (50mm), and σ_y is the yield strength of the beam material (240MPa). So M_y is obtained equal to 28.8KN.m.

The minimum bending moment required to enter the entire beam into the plastic zone (M_p) is obtained from the following equation:

$$M_p = \frac{3}{2}M_y = 43.2KN.m \qquad (9)$$

According to the obtained values for M_y and M_p and also the applied moment value (i.e., 36.8KN.m), a section of the beam cross-section enters to the plastic zone and another section remains in the elastic region. The elastic region (Y_Y) (Fig. 5) is calculated from the following equation:

$$Y_Y = c\sqrt{3 - \frac{2M}{M_y}} \tag{10}$$

Thus according to the equation (10) Y_Y is obtained equal to 40mm. The stress in the plastic zone due to the elasto-plastic properties of the beam material and its yield strength (240MPa) is obtained 240MPa. Also, the stress in the elastic zone of the beam is determined from the following equation:

$$\sigma = \frac{MY}{I} \tag{11}$$

where Y is the distance from the neutral axis (Fig. 5). So the stress distribution of the beam under the pure bending moment is resulted according to Fig. 6a.

Concerning this fact that the unloading is elastic, the released stress during unloading (σ') in the entire of the beam cross-section is given by:

$$\sigma' = -\frac{MY}{I} \tag{12}$$

Therefore, the distribution of the released stress during unloading is determined accordance to Fig. 6b. By superposition of stress distribution during loading and unloading, the residual stress distribution of the beam is obtained as shown in Fig. 6c.

5. Experimental Approach

For applying the inverse eigenstrain method in an actual part, information of ref. [5] was used. In the ref. [5] a 3 mm plate of AA6061-T6 aluminum alloy was processed by ultrasonic-assisted friction stir welding under different vibration amplitudes that in the present work, only the 2μm vibration amplitude case was considered. Since this part was relatively thin, it was expected that the distribution of the residual stress in the direction of the thickness is almost constant. Therefore, it was logical to use the 2D eigenstrain method on this part. The method of calculating residual stresses in the mentioned part using the inverse eigenstrain method was the same as in the numerical analysis section.

6. Results and Discussion

6.1. Numerical Analysis:

Fig. 7 illustrates the comparison between the obtained residual stresses from the FE simulation and analytical method. As shown in Fig. 7, there is a very good agreement between the results. This shows the accuracy of the FE simulation. It should be noted that from Fig. 7 to Fig. 10, the residual stresses are plotted in terms of distance from center of the beam cross-section ($+Y$ and $-Y$ Fig. 2).
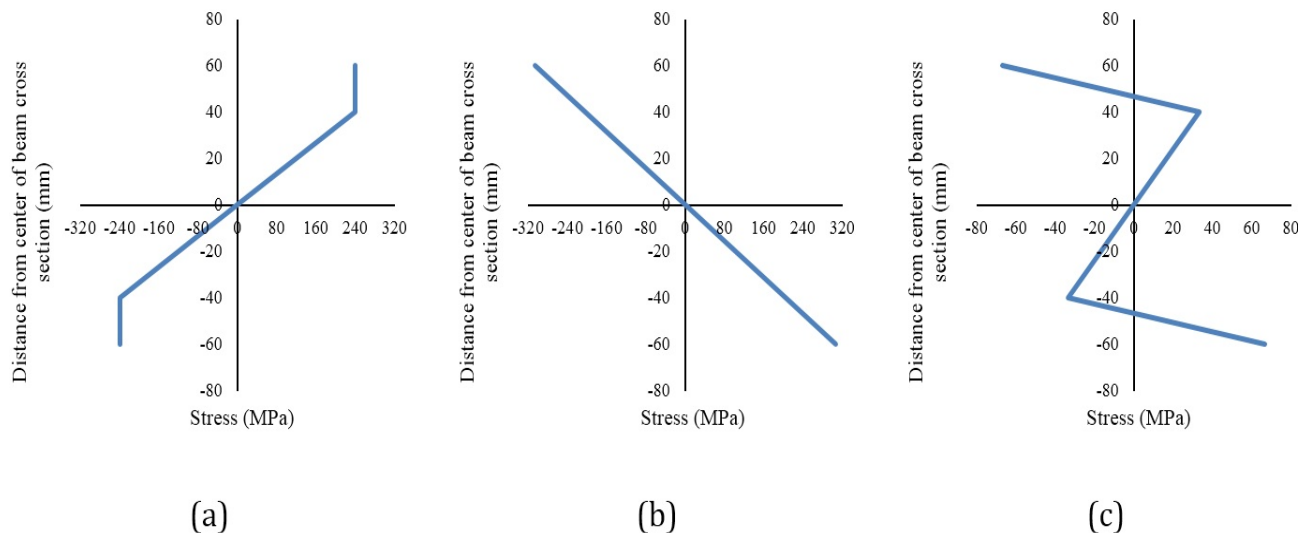

(a)   (b)   (c)

Fig. 6. The stress distribution of the beam under moment considered in this paper: a) The stress distribution of the beam under pure moment b) The released stress distribution of the beam during unloading c) The residual stress distribution of the beam after unloading.
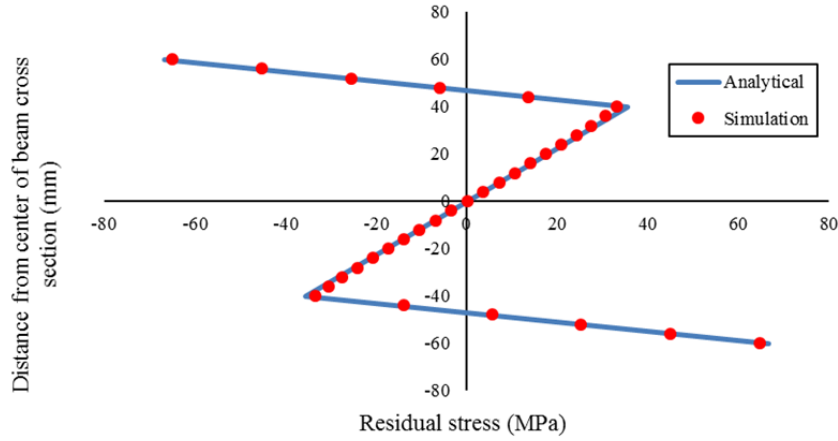
Fig. 7. Residual stress obtained from FE simulation and analytical method.
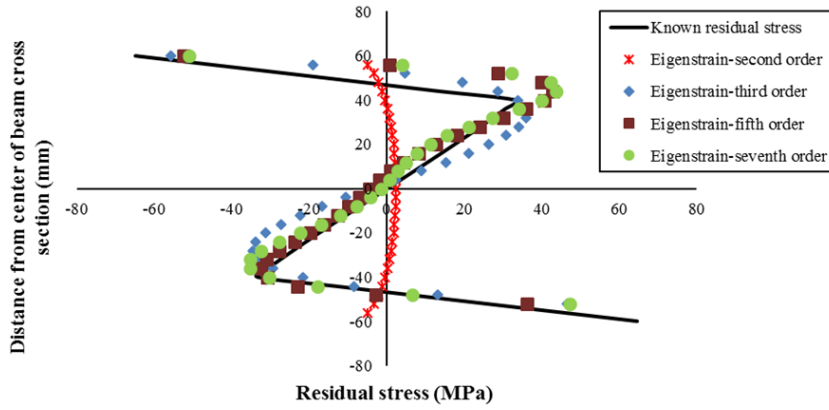

Fig. 8. Residual stress obtained from the inverse eigenstrain method for different orders of Legendre polynomials as basis functions and the known residual stress.

In Fig. 8, the obtained residual stresses from the inverse eigenstrain method are shown for different orders of Legendre polynomials as basis functions. Also, in this figure for comparison, the known residual stresses are plotted. According to the figure, for the second order of the Legendre polynomials, the obtained results are unacceptable, but with increasing the Legendre polynomial order to third order, the residual stresses are in good agreement with the known residual stresses. Additionally, with more increase in the order of Legendre polynomials to fifth and seventh orders, there is not much change in the accuracy of the results, thus the results for the fifth and seventh orders are almost consistent. Therefore, in the inverse eigenstrain method, the accuracy of the results increases with increasing the basis function order. Also, with increasing the basis function order from one order to the next, no significant change is seen in the accuracy of the results. Hence, with the excessive increase in the order of the basis functions, the accuracy of the results is not increased, only the time of calculations increases.

In Fig. 9, the obtained residual stresses by the inverse eigenstrain method are shown for the fifth order of the Legendre basis functions and different number of displacement measurement points. Also, in this figure, the known residual stresses are given for accuracy assessment of the results. It can be seen that for the number of measurement points 11 and 16, there is not very good agreement between the residual stresses obtained from the inverse eigenstrain method and the known residual stresses. Although with increasing the number of measurement points from 11 to 16, the accuracy of the results is slightly increased. However, with more increase in the number of measurement points, i.e., with 31 points, a good agreement is observed between the residual stresses obtained from the inverse eigenstrain method and the known residual stresses. Therefore, in the inverse eigenstrain method, the number of the displacement measurement points must be increased to a value until the desired accuracy in the results is attained.

Fig. 10 illustrates the obtained residual stresses from the inverse eigenstrain method for the basis functions of the Legendre polynomials and the Chebyshev polynomials. Additionally, in this figure, the known residual stresses are given for accuracy assessment of the results. According to the figure, for the Chebyshev polynomials of the fifth order, there is no good

agreement between the obtained results and the known residual stresses. Even with increasing the Chebyshev polynomials order to the seventh order, the results do not have good accuracy. For the Legendre polynomials basis functions, the results have good accuracy, even in the fifth order. Therefore, choice of the appropriate basis functions in the inverse eigenstrain method is very important. Basically, in the inverse eigenstrain method, the appropriate basis functions are selected based on the previous information from the residual stress distribution [12]. But if such information is not available, a sufficient investigation must be conducted for selecting the appropriate basis functions.

6.2. Experimental Approach

In Fig. 11, the residual stress in the z-direction (σz) for the considered actual part calculated from the 2D inverse eigenstrain method is shown for different orders of Legendre polynomials as basis functions. Also, in this figure, for investigation of the result accuracy of the inverse eigenstrain method, the residual stress obtained from contour method was plotted, which was extracted from the ref. [5]. According to the figure, for the third order of the Legendre polynomials, the results are inadmissible, but with increasing the order to fourth, the residual stress is in good agreement with the contour method results. Also, with more increase in the order to fifth, there is almost no change in the results. Therefore, for the considered actual part, the inverse eigenstrain method results with the fourth order of the Legendre polynomials are accurate. It is worth noting that according to the previous experience, the number of measuring points (200 points) was assumed to be appropriate from the beginning. Therefore, the number of measuring points was evaluated and the results have confirmed this fact. Moreover, since the relatively precise results were obtained with the basis functions of the Legendre polynomials at low orders, it does not have any other reason to test the basis functions of the Chebyshev polynomials. It should be noted that in Fig. 11 and next figure, the residual stresses are plotted in terms of distance from retreating side of the part (Ref. 24).
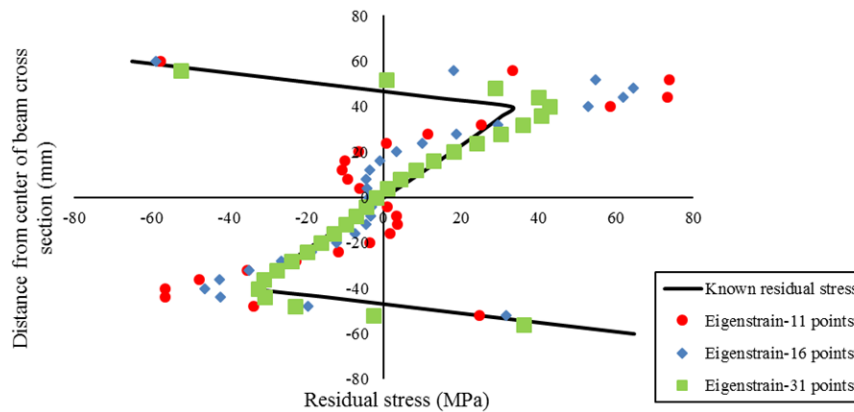

Fig. 9. Residual stress obtained from the inverse eigenstrain method for the fifth order of the Legendre basis functions and different number of displacement measurement points and the known residual stress.
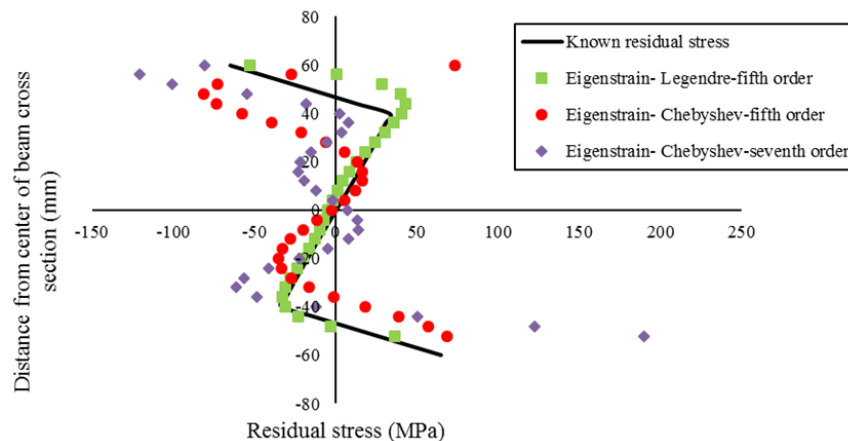

Fig. 10. Obtained residual stresses from the inverse eigenstrain method for the basis functions of the Legendre polynomials and the Chebyshev polynomials and the known residual stress.
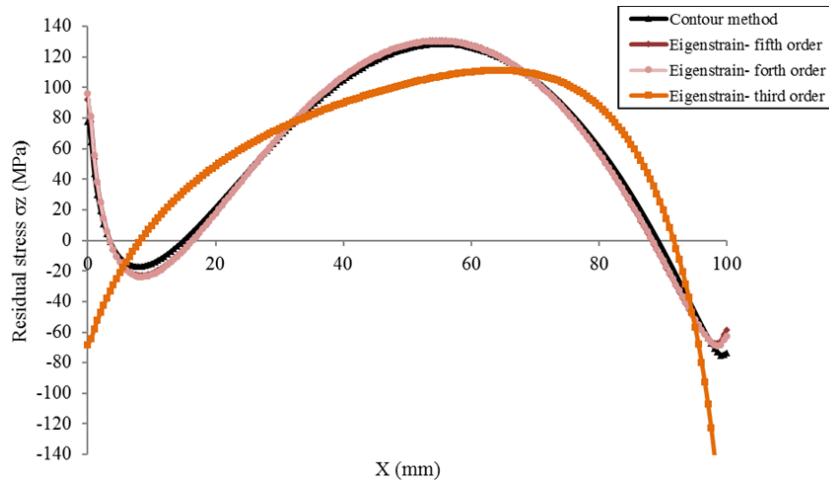
Fig. 11. Residual stresses obtained from the inverse eigenstrain method for different orders of Legendre polynomials as basis functions and the contour method for the considered actual part.
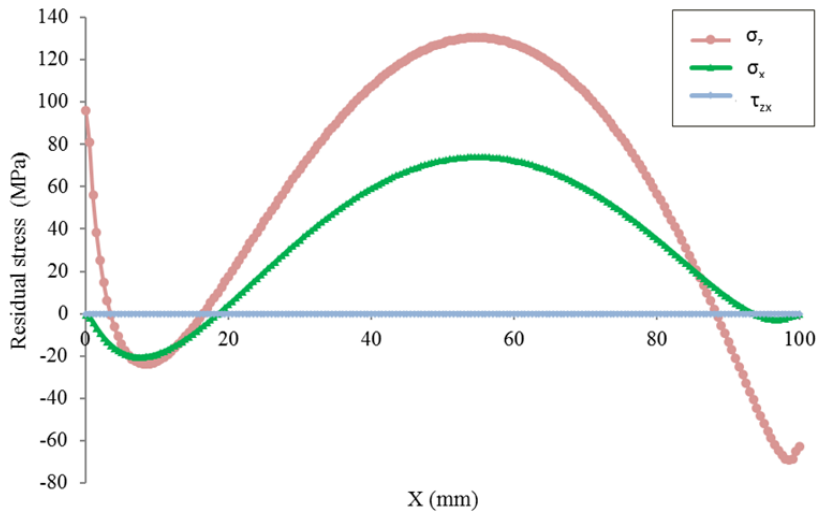

Fig. 12. Residual stress tensor components obtained from the 2D inverse eigenstrain method for the considered actual part.

As previously noted, when the eigenstrain distribution is determined, all components of the residual stress tensor can be obtained. Fig. 12 shows the residual stress tensor components obtained from the 2D inverse eigenstrain method for the considered actual part. As the figure shows, the magnitude of the transverse stress is significant. This shows the importance of the inverse eigenstrain method in relation to other methods such as contour that only give the residual stress in one direction. Also, according to the figure, the shear stress is negligible and almost zero.

7. Conclusions

In this research, a numerical experiment was performed to examine the effective parameters on the result accuracy of the inverse eigenstrain method in measuring the residual stresses. The investigated parameters include the order of the basis functions polynomials, the type of

the basis functions polynomials, and the number of displacement measurement points. Furthermore, in this work, the inverse eigenstrain method was applied for an actual part. In this study, the following results were obtained:

1. In the inverse eigenstrain method, the result accuracy increases with increasing the basis functions order. However, with the excessive increasing in the order of the basis functions, the result accuracy does not increase, but only the time of calculations increases.

2. In the inverse eigenstrain method, the numbers of displacement measurement points must be increased to a value until the desired accuracy in the results is attained.

3. The type of the basis functions is very important in the inverse eigenstrain method. So that

by selecting the appropriate basis functions, the desired accuracy can be obtained in low orders.

4. Also in the real conditions, accurate results can be obtained by selecting the appropriate parameters of the inverse eigenstrain method.

References

[1] G.S. Schajer, Practical Residual Stress Measurement Methods, John Wiley and Sons, New York, (2013).

[2] M. Sedighi, M. Honarpisheh, Investigation of cold rolling influence on near surface residual stress distribution in explosive welded multilayer, Strength. Mater., 44(6) (2012) 693-698.

[3] M. Sedighi, M. Honarpisheh, Experimental study of through-depth residual stress in explosive welded Al-Cu-Al multilayer, Mater. Design., 37 (2012) 577-581.

[4] M.B. Prime, Cross-sectional mapping of residual stress by measuring the surface contour after a cut, J. Eng. Mat. Tech., 123 (2001) 162-168.

[5] I. Alinaghian1, M. Honarpisheh, S. Amini, The influence of bending mode ultrasonic-assisted friction stir welding of Al-6061-T6 alloy on residual stress, welding force and macrostructure, Int. J. Adv. Manuf. Tech. 95 (5-8) (2018) 2757-2766.

[6] M. Kotobi, M. Honarpisheh. Experimental and numerical investigation of through-thickness residual stress of laser-bent Ti samples, J. Strain. Ana., 52(6) (2017) 347-355.

[7] M. Kotobi, M. Honarpisheh, Uncertainty analysis of residual stresses measured by slitting method in equal-channel angular rolled Al-1060 strips, J. Strain. Ana., 52(2) (2017) 83-92.

[8] M. Honarpisheh, E. Haghighat, M. Kotobi, Investigation of residual stress and mechanical properties of equal channel angular rolled St12 strips, P. I. Mech. Eng. L. J. Mat., (2016) 1-11, https://doi.org/10.1177/1464420716652436.

[9] M. Kotobi, M. Honarpisheh, Through-depth residual stress measurement of laser bent steel-titanium bimetal sheets, J. Strain. Ana., 53(3) (2018) 130-140.

[10] M. Moazzam, M. Honarpisheh, Residual stresses measurement in UIC 60 rail by ring-core method and sectioning technique, A. J. Mech. Eng., (2017) https://doi.org/10.22060/mej.2017.12879.5457.

[11] T.S. Jun, A.M. Korsunsky, Evaluation of residual stresses and strains using the eigenstrain reconstruction method, Int. J. Solid. Struct., 47 (2010) 1678-1686.

[12] S.A. Faghidian, A smoothed inverse eigenstrain method for reconstruction of the regularized residual fields, Int. J. Solid. Struct., 25 (2014) 4427-4434.

[13] M.R. Hill, Determination of residual stress based on the estimation of eigenstrain, Ph.D. Dissertation, Stanford University, (1996).

[14] A.M. Korsunsky, On the modeling of residual stresses due to surface peening using eigenstrain distributions, J. Strain. Ana., 40(8) (2005) 817-824.

[15] A.M. Korsunsky, Variational eigenstrain analysis of synchrotron diffraction measurements of residual elastic strain in a bent titanium alloy bar, J. Mech. Mater. Struct., 1(2) (2006) 259-277.

[16] A.T. DeWald, M.R. Hill, Multi-axial contour method for mapping residual stresses in continuously processed bodies, J. Exp. Mech., 46 (2006) 473-490.

[17] A.M. Korsunsky, G.M. Regino, D. Nowell, Variational eigenstrain analysis of residual stresses in a welded plate, Int. J. Solid. Struct., 44 (2007) 4574-4591.

[18] T.S. Jun, A.M. Venter, C.P. la Grange, F. Hofmann, J. Belnoue, P.R. van Heerden, A. Evans, A.M. Korsunsky, Eigenstrain analysis of non-uniformly shaped shot-peened samples, J. Procedia. Eng., 1 (2009) 151-154.

[19] X. Song, W.C. Liu, J.P. Belnoue, J. Dong, G.H. Wu, W.J. Ding, S.A.J. Kimber, T. Buslaps, A.J.G. Lunt, A.M. Korsunsky, An eigenstrain-based finite element model and the evolution of shot peening residual stresses during fatigue of GW103 magnesium alloy, Int. J. Fatigue., 42 (2012) 284-295.

[20] W.D. Musinski, D.L. McDowell, On the eigenstrain application of shot-peened residual stresses within a crystal plasticity framework: Application to Ni-base superalloy specimens, Int. J. Mech. Sci., 100 (2015) 195-208

[21] H.T. Luckhoo, T-S. Jun, A.M. Korsunsky, Inverse eigenstrain analysis of residual stresses in friction stir welds, J. Procedia. Eng., 1 (2009) 213-216.

[22] T-S. Jun, K. Dragnevski, A.M. Korsunsky, Microstructure, residual strain, and eigenstrain analysis of dissimilar friction stir welds, J. Mat. Des., 31 (2010) S121-S125.

[23] X. Song, I. Kyriakogloub, A.M. Korsunsky, Analysis of residual stresses around welds in a combustion casing, J. Procedia. Eng., 1 (2009) 189-192.

[24] M. Achinth, D. Nowell, Eigenstrain modelling of residual stresses generated by arrays of LSP shots, J. Procedia. Eng., 10 (2011) 1327-1332.

[25] M. Achinth, D. Nowell, K. Shapiro, P.J. Withers, Eigenstrain modelling of residual stress generated by arrays of Laser Shock Peeing shots and determination of the complete stress field using limited strain measurements, J. Surf. Coat. Tech., 216 (2012) 68-77.

[26] S. Coratella, M. Sticchi, M.B. Toparli, M.E. Fitzpatrick, N. Kashaev, Application of the eigenstrain approach to predict the residual stress distribution in laser shock peened AA7050-T7451 samples, J. Surf. Coat. Tech., 273 (2015) 39-49.

[27] M.E. Kartal, F.P.E. Dunne, A.J. Wilkinson, Determination of the complete microscale residual stress tensor at a subsurface carbide particle in a single-crystal superalloy from free-surface EBSD, J. Acta. Mater., 60 (2012) 5300-5310.

[28] M.E. Kartal, R. Kiwanuka, F.P.E. Dunne, Determination of sub-surface stresses at inclusions in single crystal superalloy using HR-EBSD, crystal plasticity and inverse eigenstrain analysis, Int. J. Solid. Struct., 67 (2015) 27-39.

[29] M.E. Kartal, Y.H. Kang, A.M. Korsunsky, A.C.F. Cocks, J.P. Bouchard, The Influence of welding procedure and plate geometry on residual stresses in thick components, Int. J. Solid. Struct., 80 (2015) 420-429.

[30] M. Ogawa, T. Ishii, Evaluation of the three-dimensional welding residual stresses based on the eigenstran methodology via X-ray measurements, J. Mat. Res. Proc., 2 (2016) 329-334.

[31] M.P. Fransen, Eigenstrain reconstruction of residual stresses induced by selective laser melting, MSc Thesis, Delft University, 2016.